



Journal of Groundwater Research, Vol.3, 4/1, December 2015

Entropy Theory for Groundwater Modeling

Vijay P. Singh and Huijuan Cui

Department of Biological and Agricultural Engineering &
Zachry Department of Civil Engineering
Texas A&M University
College Station, Texas 77843-2117, USA
Email: vsingh@tamu.edu

Abstract

For over two decades entropy theory has been applied to groundwater modeling with particular regard to (1) groundwater head, (2) parameter estimation, and (3) contaminant transport. Entropy theory is formulated in two domains: real domain and frequency domain. In the real domain, the theory comprises (a) Shannon entropy or another form, (2) principle of maximum entropy, (3) relative entropy, and (4) concentration theorem. The theory allows a probabilistic description in each case. In the frequency domain, it comprises Burg entropy, configurational entropy, and relative entropy. The objective of this study to review the potential of entropy theory in groundwater hydrology, point out its limitations, and suggest directions for future work. Observed groundwater depth measured from the land surface were used to evaluate the entropy theories. It was found that hourly groundwater level showed significant daily periodicity. The largest spectral peak happened at $1/24^{\text{th}}$ frequency, which was determined by the relative entropy spectral analysis with the highest resolution among the three entropies. For modeling groundwater level, both configurational entropy and relative entropy fitted observations well, and the errors were much smaller than for the Burg entropy.

Keywords: Entropy theory, spectral analysis, Burg entropy, relative entropy, configurational entropy, groundwater

1. Introduction

The entropy theory has been widely applied in surface water hydrology (Singh, 1997; Singh, 2011; Singh et al., 2007), but its application has been limited in groundwater hydrology. Entropy theory can be formulated both in real domain and in frequency domain. In the real domain, the entropy theory allows a probabilistic description of each groundwater variable. In the 1990s, the principle of maximum entropy (Jaynes, 1957a; Jaynes, 1957b) was applied to estimate the groundwater flow head distribution (Barbe et al., 1994) using the Shannon entropy (Shannon, 1948), and the relative entropy theory was applied for forward groundwater modeling and solving inverse problems (Woodbury and Ulrych, 1993; Woodbury and Ulrych, 1996; Woodbury and Ulrych, 1998). In the frequency domain, the entropy theory connects the spectral analysis and time series analysis of groundwater. However, the entropy theory does not seem to have been applied to groundwater time series analysis.

Burg (1967; 1975) developed what is now referred to as the Burg entropy spectral analysis (BESA) in which he linked the entropy theory to spectral analysis and time series analysis. It not only improved the resolution of spectral density but also improved the reliability of time series modeling. BESA has been applied to forecast streamflow and has been shown to be preferable to classical methods (Krstanovic and Singh, 1989; Krstanovic and Singh, 1991a; Krstanovic and Singh, 1991b; Singh, 2013). Besides the Burg entropy, the configurational entropy spectral analysis (CESA), introduced by Frieden (1972) and Gull and Daniell (1978), is another maximum entropy spectral analysis (Katsakos-Mavromichalis et al., 1985; Tzannes et al., 1985; Tzannes and Avgeris, 1981). Cui and Singh (2015) have developed the theory of configurational entropy spectral analysis

(CESA). Superior to the Burg entropy spectral analysis (BESA), CESA has been shown to be not restricted to the autoregressive (AR) process (Liefhebber and Boeke, 1987; Ortigueira et al., 1981).

There is also relative entropy spectral analysis (RESA), which was developed by Shore (1979; 1981) as an extension of Burg's maximum entropy spectral analysis, where the spectral power was considered as a random variable. Later, another version of RESA was developed by Tzaneess et al. (1985), considering frequency as a random variable. The RESA spectra are reported to have higher resolution and are more accurate in detecting peak location than other methods for spectral computation (Papademetriou, 1998). Besides, the RESA theory reduces the number of prediction coefficients by relying on the prior information (Schroeder, 1982).

However, the above entropy spectral analyses have been applied to surface streamflow time series, but have not yet been used to groundwater time series. The objective of this study is to develop three entropy-based spectral analyses for modeling hourly groundwater data, and to see which entropy approach performs the best for forecasting groundwater level.

2. Methods

Let the groundwater level time series $y(t)$ be denoted as y_1, y_2, \dots, y_T , where T is the total number of time series. To apply the entropy spectral analysis, the groundwater time series is transferred to the frequency (f) domain, and the information on groundwater series is stored in the spectral density $p(f)$. Considering frequency f as a random variable, the normalized spectral density $p(f)$ can be taken as the probability density function. Then, the uncertainty of groundwater level in terms of spectral density can be determined by the Burg entropy, configurational entropy and relative entropy.

First, the Burg entropy can be defined as

$$H_B(f) = - \int_{-W}^W \ln[p(f)]df \quad (1)$$

where p is the spectral density function, f is the frequency that varies from $-W$ to W , $W=1/(2\Delta t)$ is the Nyquist fold-over frequency, Δt is the sampling period, which is hour in this study. It is observed that the Burg entropy is defined as the sum of log of the spectral density.

Taking the expectation of the integral of the log of spectral density, the configurational entropy is defined as

$$H_C(f) = - \int_{-W}^W p(f) \ln[p(f)]df \quad (2)$$

On the other hand, with given prior spectral density $q(f)$, the relative entropy of the spectral density $p(f)$ can be defined as

$$H_R(f) = \int p(f) \ln[p(f)/q(f)]df \quad (3)$$

The prior spectral density can be taken as a background noise with the peak assumed at the observed periodicity. It is noted that when a uniform prior is taken, the relative entropy reduces to the configurational entropy.

The development of entropy spectral analyses comprises the following steps: (1) derivation of entropy-based spectral density, (2) computation of the Lagrange multipliers, (3) estimation of autocorrelation function, and (4) modeling groundwater level.

2.1 Derivation of Entropy-Based Spectral Density

To obtain the least-biased spectral density, one needs to maximize (minimize) the Burg entropy and configurational entropy or relative entropy, subject to specified constraints. The constraints can be formed from the relationship between the spectral density and autocorrelation. Using the first N lags of autocorrelation, the constraint is written as

$$\rho_n = \int_{-W}^W p(f) e^{i2\pi f n \Delta t} df, \quad -N \leq n \leq N \quad (4)$$

where $i = \sqrt{-1}$ and ρ_n is the autocorrelation function of n -th lag. When $n=0$, equation (4) reduces to

$$\rho_0 = \int_{-W}^W p(f) df = 1 \quad (5)$$

Thus, entropy can be maximized or minimized with the use of Lagrange multipliers. The Lagrangian function can be formulated as

$$L(f) = H(f) - \sum_{n=-N}^N \lambda_n \left[\int_{-W}^W p(f) \exp(i2\pi f n \Delta t) df - \rho_n \right] \quad (6)$$

where $\lambda_n, n=0, 1, 2, \dots, N$, are the Lagrange multipliers, and $H(f)$ is the entropy to be maximized [as $H_B(f)$ or $H_C(f)$] or to be minimized [as $H_R(f)$]. Taking the partial derivative of $L(f)$ with respect to the spectral density and equating to zero, $\frac{\partial L(f)}{\partial p(f)} = 0$, the least-biased spectral densities obtained

from the maximization of the Burg entropy or configurational entropy and from the minimization of the relative entropy, respectively, are

$$p_B(f) = \frac{1}{\sum_{n=-N}^N \lambda_n e^{-i2\pi f n \Delta t}} \quad (7)$$

$$p_C(f) = \exp\left(-1 - \sum_{n=-N}^N \lambda_n e^{i2\pi f n \Delta t}\right) \quad (8)$$

$$p_R(f) = q(f) \exp\left(-1 - \sum_{n=-N}^N \lambda_n e^{i2\pi f n \Delta t}\right) \quad (9)$$

It can be seen from the above three equations that the spectral density derived from the Burg entropy is in the form of inverse of polynomials, while the ones from the configurational entropy and relative entropy are in the exponential form. The form in equation (7) suggests that BESA is related to the linear process.

2.2 Determination of Lagrange Multipliers

The ways for determining Lagrange multipliers are different as the formulation of entropy-based spectral densities obtained above are different. For the Burg entropy, the Lagrange multipliers can be computed from the Levinson-Burg algorithm developed by Burg (1967; 1975). The Levinson-Burg algorithm is a recursive algorithm for estimating model parameters, and improves the original Levinson algorithm by computing forward and backward prediction error together to update the coefficient of next order (Collomb, 2009; Lin and Wong, 1990).

On the other hand, to compute the parameters of the configurational entropy and relative entropy approach, the cepstrum analysis needs to be incorporated. For the relative entropy approach, taking the inverse Fourier transform of the log-magnitude of equation (9), one obtains

$$\int_{-W}^W \{1 + \log[p(f)] - \log[q(f)]\} e^{i2\pi f n \Delta t} df = \int_{-W}^W \left(-\sum_{n=-N}^N \lambda_n e^{i2\pi f n \Delta t}\right) e^{i2\pi f n \Delta t} df \quad (10)$$

It can be seen from equation (10) that there are two terms relating to the spectral density that can turn to the cepstrum of autocorrelation, which is also called autocepstrum.

Let the prior cepstrum of autocorrelation be denoted as $e_q(n)$, which is transformed from the prior spectral density as

$$e_q(n) = \int_{-W}^W \log q(f) e^{i2\pi fn\Delta t} df \quad (11)$$

Similarly, the posterior cepstrum of autocorrelation $e_p(n)$ transform from the posterior spectral density can be expressed as

$$e_p(n) = \int_{-W}^W \log p(f) e^{i2\pi fn\Delta t} df \quad (12)$$

Doing the integration of both sides of equation (10), one gets

$$\delta_n + e_p(n) - e_q(n) = - \sum_{s=-N}^N \lambda_s \delta_{n-s} \quad (13)$$

where δ_n is the delta function defined as:

$$\delta_n = \begin{cases} 1, & n = 0 \\ 0, & n \neq 0 \end{cases} \quad (14)$$

Equation (13) can be expanded as a set of N linear equations:

$$\begin{aligned} \lambda_0 &= -1 - e_p(0) + e_q(0) \\ \lambda_1 &= -e_p(1) + e_q(1) \\ &\vdots \\ \lambda_k &= -e_p(k) + e_q(k) \end{aligned} \quad (15)$$

Equation (15) enables to solve for the Lagrange multipliers in a straight-forward manner. Thus, the Lagrange multipliers can be estimated from the summation of the prior and posterior autocepstrums. The prior autocepstrum can be estimated from the observed periodicity of hourly groundwater level, while the posterior autocepstrum can be estimated from the following recursive function introduced by Nadeu (1992) as

$$e_p(n) = 2[\rho(n) - \sum_{k=1}^{n-1} \frac{k}{n} e_p(k) \rho(n-k)], \quad n > 0 \quad (16)$$

It is seen from equation (16) that the n th lag of cepstrum $e_p(n)$ is dependent on the previous $n-1$ lags of cepstrum and n -lags of autocorrelation. Thus, for given N lag autocorrelations, the cepstrum of autocorrelation can be computed up to lag N .

For the configurational entropy approach, which is equivalent to the relative entropy without a prior, the cepstrum e_q in equation (15) equals 0 and diminishes, and the Lagrange multipliers are solved from

$$\begin{aligned} \lambda_0 &= -1 - e_p(0) \\ \lambda_1 &= -e_p(1) \\ &\vdots \\ \lambda_k &= -e_p(k) \end{aligned} \quad (17)$$

where $e_p(n)$ is computed from equation (16) as well.

2.3 Autocorrelation function

Following Burg's (1967; 1975) derivation, maximization of the Burg entropy allows the autocorrelation to be estimated as a linear combination of previous lags as

$$\rho_{N+k} = -\sum_{j=1}^m \rho_{N+k-j} a_j \quad (18)$$

where parameters a_j are computed from the Levinson-Burg algorithm.

On the other hand, for the configurational entropy and relative entropy, the autocorrelation is estimated with the inverse relationship of equation (16) using the autocepstrum as

$$\rho_{N+k} = \frac{e_p(N+k)}{2} + \sum_{j=1}^m \frac{k}{N+k} e_p(j) \rho(N+k-j) \quad (19)$$

When no prior is given, equation (19) reduces to

$$\rho_{N+k} = \sum_{j=1}^m \frac{k}{N+k} e(j) \rho(N+k-j) \quad (20)$$

2.4 Modeling

Groundwater level \hat{y}_t is modeled from m previous observed values y_k in the same manner as autocorrelation function is estimated. Thus, using BESA, groundwater level can be modeled by a linear combination of past series weighted by the coefficients in equation (18) to extend the autocorrelation, which becomes

$$\hat{y}_t = a_1 y_{t-1} + a_2 y_{t-2} + \dots + a_m y_{t-m} \quad (21)$$

When using CESA or RESA, groundwater level is modeled with cepstrum analysis, in the same way as autocorrelation is estimated. Thus, groundwater level can be modeled as

$$\hat{y}_t = \frac{c_p(t)}{2} + \sum_{j=1}^m \frac{k}{t} c_q(j) y(t-j) \quad (22)$$

where $c(j)$ is the cepstrum of the time series and equals to $\frac{1}{2} e(n)$. Then equation (22) can be written as

$$\hat{y}_t = \frac{1}{4} e_p(t) + \frac{1}{2} \sum_{j=1}^m \frac{k}{t} e_q(j) y(t-j) \quad (23)$$

When no prior is given, e_p is 0, thus, groundwater level forecasted by CESA becomes

$$y_t = \frac{1}{2} \sum_{j=1}^m \frac{k}{t} e(j) y(t-j) \quad (24)$$

3. Application

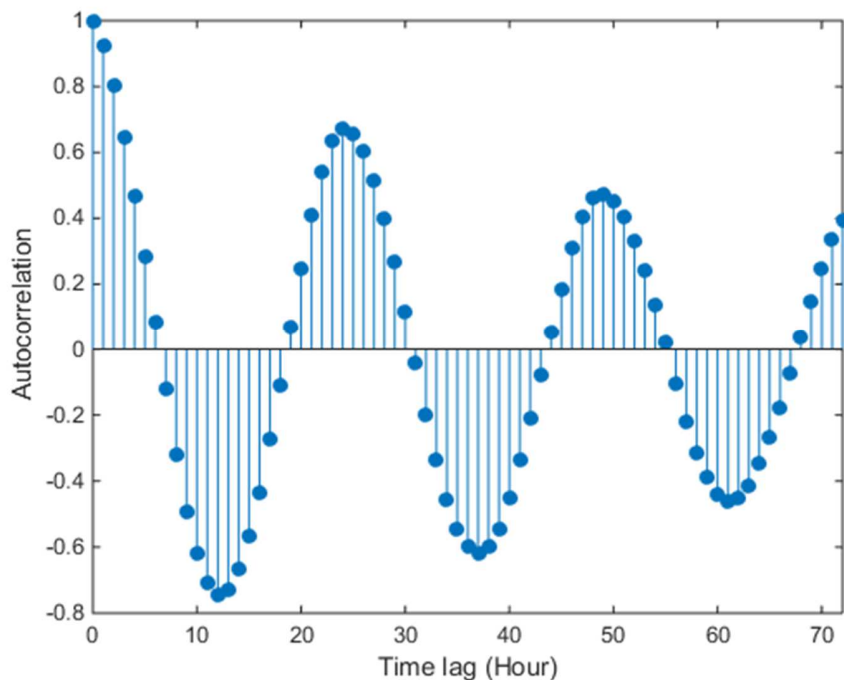
The proposed three entropy spectral analysis methods, BESA, CESA and RESA, were verified using hourly groundwater level data during December 2014, obtained from the U.S. Geological Survey (USGS). The groundwater level was estimated by the depth of water level from the land surface. Four stations, as shown in Table 1, were chosen from different locations to evaluate the application of the proposed methods. Lomaroste well was constructed in the South Coast aquifer (Puerto Rico), and the depth of well is unknown but the hole is 70.0 feet below land surface. Addicks piezometer and Wayne wells were both constructed in the "Coastal lowlands aquifer system." The well depth of Addicks piezometer is 237 ft, and that of Wayne was 82 ft. The last Gideon well was constructed in the "Mississippi embayment aquifer system," and depth of well and hole were both 1330 ft.



Table 1. Summary of groundwater levels.

| Name | Station No. | Location | Mean (ft) | Variance (ft ²) | CV | Trend |
|--------------------|-----------------|-----------------------------|-----------|-----------------------------|-------|-------------------------|
| Lomaroeste well | 175734066233300 | Santa Isabel, PR | 16.321 | 0.081 | 0.017 | $y = 0.0014t + 15.929$ |
| Addicks piezometer | 294726095351104 | Harris county, Texas | 164.120 | 0.037 | 0.001 | $y = -0.0002t + 164.29$ |
| Wayne | 314115088392301 | Wayne county, Mississippi | 26.147 | 0.007 | 0.003 | $y = -0.0001t + 26.217$ |
| Gideon | 362718089552301 | New madrid county, Missouri | 1.618 | 0.424 | 0.402 | $y = -0.0002t + 2.1779$ |

It was noted that hourly groundwater level time series was not stationary. As shown in Table 1, an increasing trend was found at Lomaroeste well, but the other three wells showed a decreasing trend. Thus, to apply entropy spectral analysis, the trend was removed first. The autocorrelation of the trend-removed time series was plotted, as shown in Figure 1. It is seen from the figure that the autocorrelation of the groundwater level fluctuated with a 24-hour periodicity. Considering ± 0.1 as the 90% confidence interval, autocorrelation at most lags was significant.



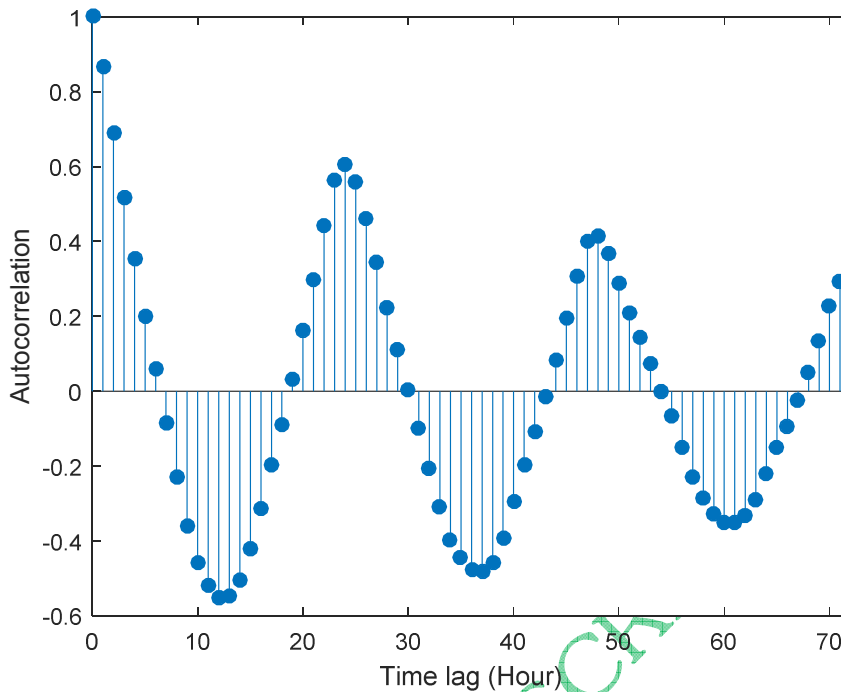


Figure 1. Plot of autocorrelation function of (a) Lomaroeste well and (b) Gideon.

3.1 Estimation of Spectral density

The spectral densities, estimated by BESA, CESA and RESA, were compared to the one estimated from the Fast Fourier transform (FFT), as plotted in Figure 2. In Both Figure 2(a) and 2(b), the spectral density has peaks at 1/24th frequency, which agrees with the 24 hour periodicity observed from the autocorrelation plot. However, the ones estimated from the entropy spectral analyses did not capture the 1/24th peak. For Lomaroeste well, BESA estimated spectral peak at 1/12th frequency. Besides, the spectral density estimated from FFT is uni-peak condition. But the ones estimated using BESA had multiple peaks. In general, the spectral density estimated from RESA was the closest to the one by FFT, as shown in the figure. Furthermore, the performance of the three entropy spectral analyses was evaluated by the Itakura-Saito distortion, which is a measure of the perceptual difference between an original spectrum and its estimate. The distortion was defined as

$$D_{I-S}(\hat{p}(f), p(f)) = \frac{1}{2\pi} \int \left[\frac{p(f)}{\hat{p}(f)} - \log\left(\frac{p(f)}{\hat{p}(f)}\right) - 1 \right] df \quad (25)$$

where $p(f)$ represents the spectral density from FFT and $\hat{p}(f)$ is the estimated spectral density. The smaller value represents a better fit. As shown in Table 2, the I-S distance value is the smallest for RESA, followed by CESA and BESA, respectively.

Table 2 Itakura-Saito distance of estimated spectral density.

| Name | BESA | CESA | RESA |
|--------------------|--------|--------|--------|
| Lomaroeste well | 20.368 | 9.435 | 5.948 |
| Addicks piezometer | 29.058 | 16.257 | 9.054 |
| Wayne | 35.126 | 22.582 | 15.224 |
| Gideon | 16.258 | 9.538 | 7.368 |

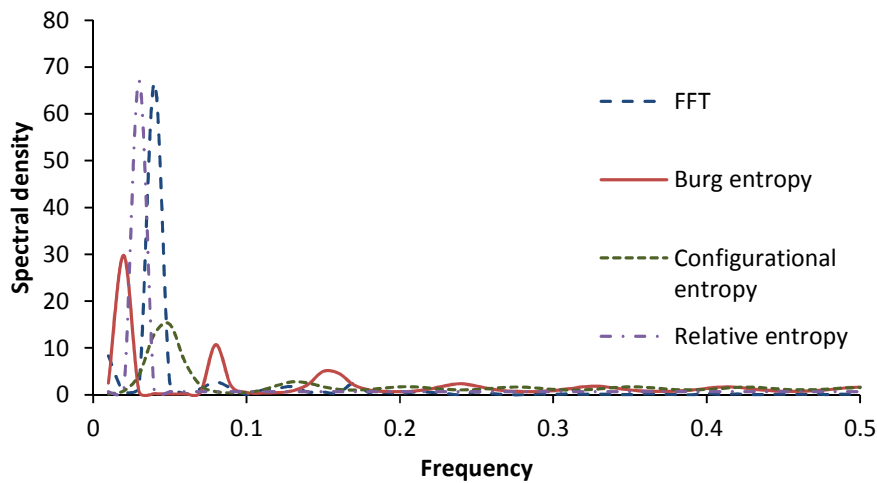
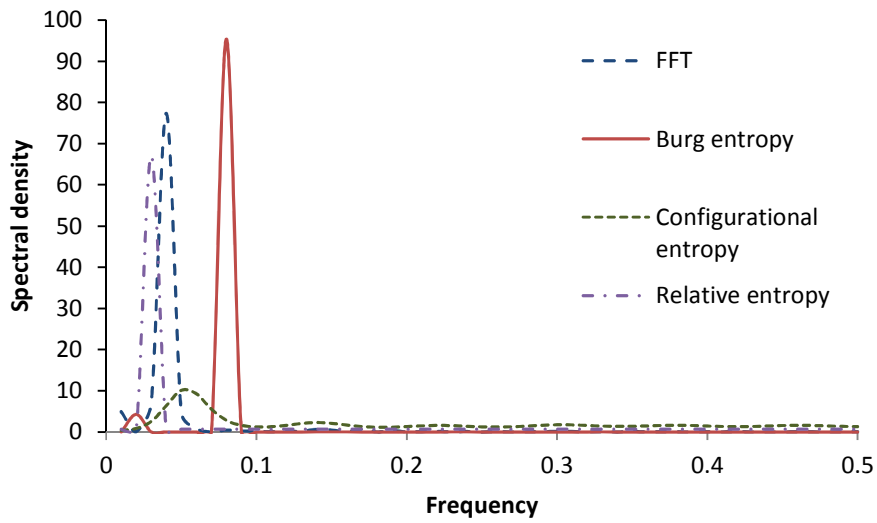


Figure 2. Estimated spectral density of (a) Lomaroste well and (b) Gideon.

3.2 Modeling groundwater level

For groundwater level time series of T period long, the first $T/2$ series data was used to estimate model parameters, and the last $T/2$ data was used to evaluate the model. The goodness of fit was examined by root mean square error ($RMSE$), coefficient of determination (r^2) and Nash-Sutcliffe efficiency (NSE), which are defined as

$$RMSE = \sqrt{\frac{\sum_{i=1}^N (\hat{y}(i) - y(i))^2}{N-1}} \quad (26)$$

$$r^2 = \left\{ \frac{\sum_{i=1}^N (y(i) - \bar{y})(\hat{y}(i) - \bar{\hat{y}})}{\left[\sum_{i=1}^N (y(i) - \bar{y})^2 \right]^{0.5} \left[\sum_{i=1}^N (\hat{y}(i) - \bar{\hat{y}})^2 \right]^{0.5}} \right\}^2 \quad (27)$$

$$NSE = 1 - \frac{\sum_{i=1}^N |y(i) - \hat{y}(i)|^j}{\sum_{i=1}^N |y(i) - \bar{y}|^j} \quad (28)$$

where $y(i)$ is the i -th observed groundwater level; $\hat{y}(i)$ is the i -th modeled groundwater level; and \bar{y} and $\bar{\hat{y}}$ are the average values of observed and computed groundwater levels, respectively. Table 2 summarizes measures of goodness of fit of modeled groundwater level. In general, the groundwater level modeled by RESA showed the smallest errors while the one by BESA showed the largest errors. It is noted that both CESA and RESA had r^2 higher than 0.65 in all four stations, and the values were similar for these two approaches.

Table 2. Model errors

| Station | Method | RMSE (ft) | r^2 | NSE |
|--------------------|--------|-----------|-------|-------|
| Lomaroeste well | BESA | 0.043 | 0.247 | 0.132 |
| | CESA | 0.016 | 0.896 | 0.700 |
| | RESA | 0.013 | 0.933 | 0.747 |
| Addicks piezometer | BESA | 0.235 | 0.258 | 0.178 |
| | CESA | 0.102 | 0.852 | 0.823 |
| | RESA | 0.093 | 0.917 | 0.815 |
| Wayne | BESA | 0.178 | 0.294 | 0.211 |
| | CESA | 0.123 | 0.675 | 0.538 |
| | RESA | 0.109 | 0.699 | 0.628 |
| Gideon | BESA | 0.161 | 0.389 | 0.234 |
| | CESA | 0.037 | 0.968 | 0.844 |
| | RESA | 0.044 | 0.954 | 0.795 |

In Figure 3, the modeled groundwater levels were plotted against the observed values. The modeled groundwater levels by BESA were farther apart from the observations. The modeled groundwater level by BESA showed smaller variance than did observations. BESA did not reach the peak level of each day as shown in Figure 3(a), and overestimated the lowest level of each day in Figure 3(b). However, both CESA and RESA fitted the observations well in both figures. Most of the time, the groundwater levels modeled by CESA and RESA were similar, which were hard to distinguish in the figure. It suggests that though the resolution in estimating the spectral density was much higher using RESA, the advantage in modeling ground water level is not that significant.

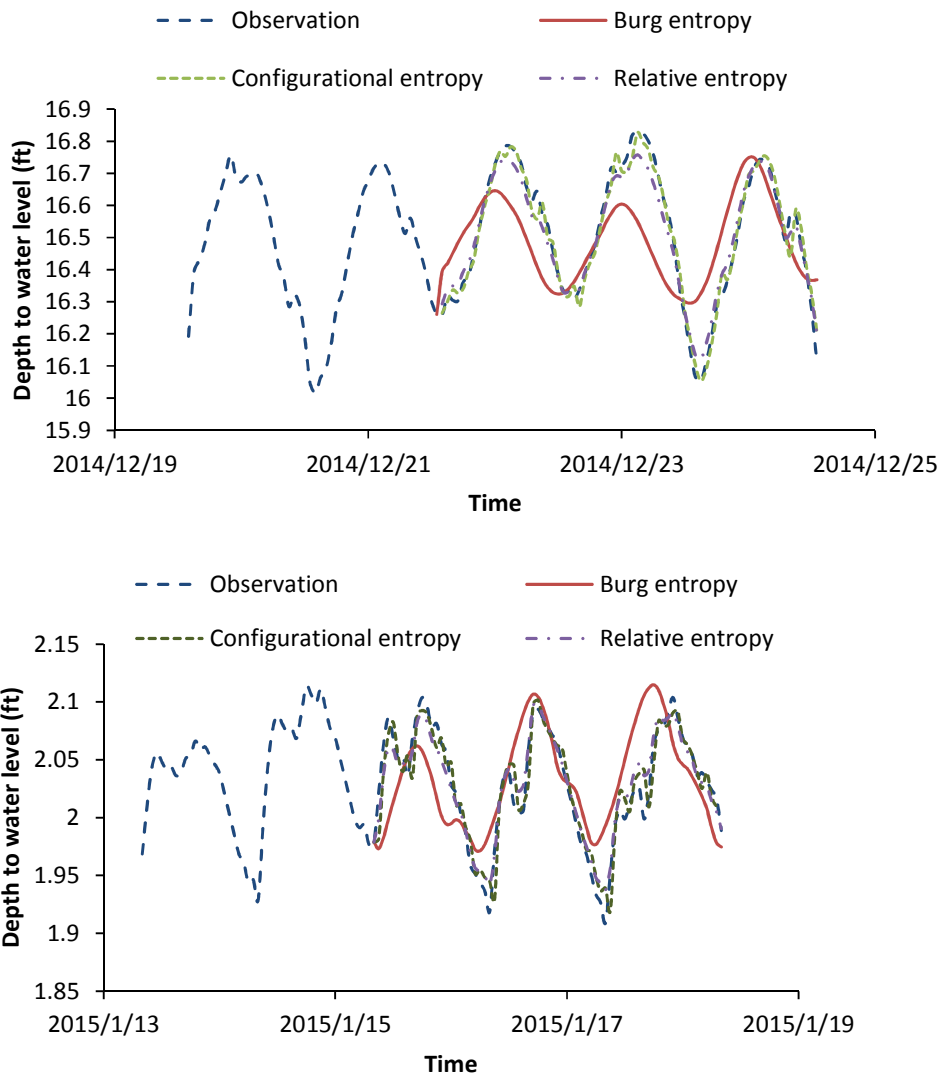


Figure 3. Modeled groundwater level of (a) Lomaroste well and (b) Gideon.

4. Conclusion

The entropy theory is applied to groundwater level after removing trend. Three entropy spectral analysis methods using Burg entropy, configurational entropy and relative entropy, are developed for groundwater level modeling. Hourly groundwater time series that were used show significant daily periodicity and possess the largest spectral peak at $1/24^{\text{th}}$ frequency. The relative entropy spectral analysis yields the highest resolution in estimating the spectral density of observed groundwater level. However, estimated spectral densities of all the three methods do not exactly follow the one from FFT and estimated spectral peaks are shifted. For modeling groundwater level, both CESA and RESA fit observations well, and the errors are much smaller than that of BESA. However, the advantage of RESA over CESA in spectral estimation is not reflected in the final model results. Further studies should be conducted for non-stationary groundwater level time series without removing trend.



References

- Barbe, D.E., F., C.J., Singh, V.P., 1994. Derivation of a distribution for the piezometric head in groundwater flow using entropy. In: Hipel, K.W. (Ed.), *Stochastic and Statistical Methods in Hydrology and Environmental Engineering*. Kluwer Academic Publishers, Netherlands.
- Burg, J.P., 1967. Maximum entropy spectral analysis, *Proceedings of 37th Meeting of Society Exploration Geophysics*, pp. 34-41.
- Burg, J.P., 1975. Maximum entropy spectral analysis. Ph.D. Thesis, Stanford University, 123 pp.
- Collomb, C., 2009. Burg's method, algorithm and recursion.
- Frieden, B.R., 1972. Restoring with maximum likelihood and maximum entropy. *J Opt Soc Am*, 62(4): 511-&.
- Gull, S.F., Daniell, G.J., 1978. Image-reconstruction from incomplete and noisy data. *Nature*, 272(5655): 686-690.
- Jaynes, E.T., 1957a. Information theory and statistical mechanics .2. *Phys Rev*, 108(2): 171-190.
- Jaynes, E.T., 1957b. Information theory and statistical mechanics.1. *Phys Rev*, 106(4): 620-630.
- Katsakos-Mavromichalis, N.A., Tzannes, M.A., Tzannes, N.S., 1985. Frequency resolution: A comparative study of four entropy methods. *Kybernetes*, 15(1): 25-32.
- Krstanovic, P.F., Singh, V.P., 1989. An entropy based method for flood forecasting, *New Directions for Surface Water Modeling (Proceedings of the Baltimore Symposium, May 1989)*. IAHS Publ.
- Krstanovic, P.F., Singh, V.P., 1991a. A univariate model for long-term streamflow forecasting .1. Development. *Stoch Hydrol Hydraul*, 5(3): 173-188.
- Krstanovic, P.F., Singh, V.P., 1991b. A univariate model for long-term streamflow forecasting .2. Application. *Stoch Hydrol Hydraul*, 5(3): 189-205.
- Liefhebber, F., Boekee, D.E., 1987. Minimum information spectral-analysis. *Signal Process*, 12(3): 243-255.
- Lin, D.M., Wong, E.K., 1990. A survey on the maximum entropy method and parameter spectral estimation. *Physics Reports*, 193(2): 41-135.
- Nadeu, C., 1992. Finite length cepstrum modeling - a simple spectrum estimation technique. *Signal Process*, 26(1): 49-59.
- Ortigueira, M.D., Garcia-Gomes, R., Tribolet, J.M., 1981. An iterative algorithm for maximum flatness spectral analysis, *International Conference on Digital Signal Processing*, Florence, Italy, pp. 810-818.
- Papademetriou, R.C., 1998. Experimental comparison of two information-theoretic spectral estimators. *Signal Processing Proceedings, 1998. ICSP '98. 1998 Fourth International Conference*, pp. 141-144 vol.1.
- Schroeder, M.R., 1982. Linear prediction, external entropy and prior information in speech signal analysis and synthesis. *Speech Communication*, 1(1): 9-20.
- Shannon, C.E., 1948. A mathematical theory of communication. *At&T Tech J*, 27(4): 623-656.
- Shore, J.E., 1979. Minimum cross-entropy spectral analysis, *Naval Research laboratory*, Washington, D. C.
- Shore, J.E., 1981. Minimum cross-entropy spectral-analysis. *Ieee T Acoust Speech*, 29(2): 230-237.
- Singh, V.P., 1997. The use of entropy in hydrology and water resources. *Hydrol Process*, 11(6): 587-626.
- Singh, V.P., 2011. Hydrologic synthesis using entropy theory: review. *J Hydrol Eng*, 16(5): 421-433.
- Singh, V.P., 2013. Entropy spectral analyses, *Entropy Theory and its Application in Environmental and Water Engineering*. John Wiley & Sons, Ltd, pp. 436-491.
- Singh, V.P., Jain, S.K., Tyagi, A., 2007. Entropy theory and its applications in risk analysis, *Risk and Reliability Analysis*, pp. 356-391.



Journal of Groundwater Research, Vol.3, 4/1, December 2015

- Tzannes, M.A., Politis, D., Tzannes, N.S., 1985. A general method of minimum cross-entropy spectral estimation. *Ieee T Acoust Speech*, 33(3): 748-752.
- Tzannes, N.S., Avgeris, T.G., 1981. A new approach to the estimation of continuous spectra. *kybernetes*, 10(2): 123-133.
- Woodbury, A.D., Ulrych, T.J., 1993. Minimum relative entropy - forward probabilistic modeling. *Water Resour Res*, 29(8): 2847-2860.
- Woodbury, A.D., Ulrych, T.J., 1996. Minimum relative entropy inversion: Theory and application to recovering the release history of a groundwater contaminant. *Water Resour Res*, 32(9): 2671-2681.
- Woodbury, A.D., Ulrych, T.J., 1998. Minimum relative entropy and probabilistic inversion in groundwater hydrology. *Stoch Hydrol Hydraul*, 12(5): 317-358.

Corresponding Author

Vijay P Singh

Department of Biological and Agricultural Engineering &
Zachry Department of Civil Engineering
Texas A&M University
College Station, Texas 77843-2117, USA
Email: vsingh@tamu.edu

ACCEPTED MANUSCRIPT - JGWR